Enzymatically produced nanocellulose as emulsifier for Pickering emulsion

Jingwei Cui[a,c], Mokarram Hossain [b], Zaigui Wang[a,*], and Chunyu Chang[c,*]

[a] *School of Life Science, Anhui Agricultural University, Hefei 230036, Anhui, China*

[b] *Zienkiewicz Centre for Computational Engineering, College of Engineering, Swansea University, Swansea, UK*

[c] *College of Chemistry and Molecular Sciences, Engineering Research Center of Natural Polymer-based Medical Materials in Hubei Province, and Laboratory of Biomedical Polymers of Ministry of Education, Wuhan University, Wuhan, 430072, Hubei, China*

Corresponding author:

Prof. Zaigui Wang

Email: wangzaigui2013@163.com (Z. Wang)

Prof. Chunyu Chang

Email: changcy@whu.edu.cn (C. Chang)

ORCID: 0000-0002-3531-5964 (C. Chang)

Abstract

With the increasing demand for label-friendly emulsion products, chemical treatments and the addition of non-natural ingredients are inadvisable in food, cosmetic, and pharmaceutical sectors. The current research proposed a green development strategy from nanocellulose production to emulsion preparation, i.e., enzymatically prepared nanocellulose (ENC) for stabilizing O/W Pickering emulsions. Benefiting from a mild enzymatic reaction, ENC inherently had low Zeta potential and oil/water interfacial tension, facilitating the formation of stable Pickering emulsions. Biphasic fluorescence staining, emulsion polymerization, and rheology were employed to investigate the emulsification characteristics of ENC, establishing the interfacial adsorption behavior and concentration-dependent phase behavior of ENC-stabilized Pickering emulsions. Importantly, due to strong particle-particle and interface-particle interactions dominated by van der Waals forces and hydrogen bonding, ENC-stabilized Pickering emulsions exhibited excellent stability under different temperatures, pH values, NaCl concentrations, and centrifugation. This work provides a green pathway for the development of nanocellulose-based Pickering emulsions.

Keywords: Nanocellulose, enzymatic hydrolysis, Pickering emulsions, phase behavior, interfacial tension

1. Introduction

The efficient adsorption of colloidal particles at the phase interface instead of conventional low-molecular-weight surfactants contributes to the formation of so-called Pickering emulsions (Low, Siva, Ho, Chan, & Tey, 2020), which have received extensive attention and have been utilized in the fields of cosmetics (Perrin, Gillet, Gressin, & Desobry, 2020), food products (Guo, Cui, & Meng, 2023; Q. Li, et al., 2021), pharmaceuticals (Albert, et al., 2019), interfacial catalysis (Ni, Yu, Wei, Liu, & Qiu, 2022), and composite materials (B. Wu, et al., 2021). Colloidal emulsifiers are mainly divided into inorganic colloidal particles (e.g., silica, clays, and calcium carbonate) (Binks, Philip, & Rodrigues, 2005; Brunier, Sheibat-Othman, Chniguir, Chevalier, & Bourgeat-Lami, 2016; Cui, Shi, Cui, & Binks, 2008) and organic colloidal particles (e.g., block copolymer micelles, proteins, and nanocellulose) (Jiao, Shi, Wang, & Binks, 2018; Kedzior, Gabriel, Dube, & Cranston, 2021; Laredj-Bourezg, Bolzinger, Pelletier, & Chevalier, 2017). Notably, nanocellulose is rapidly rising as a promising class of high mechanical strength, high surface activity, biocompatible, biodegradable, sustainable, and renewable nanomaterial, which has been extensively utilized in the development of stable functionalized interfaces and emulsion systems (Bertsch & Fischer, 2020; Parajuli & Urena-Benavides, 2022). The diverse preparation methods of nanocellulose largely determine the emulsions with different degrees of creaming, flocculation or coalescence phenomena, as well as different stabilities when subjected to changes in the external environment, such as electrolyte concentration, temperature, etc.

Cellulose nanocrystals (CNCs) prepared by sulfuric acid hydrolysis of cellulose

are commonly utilized as nanocellulose-based Pickering emulsifiers, but the electrostatic barrier formed by sulfate half ester groups on the surface hindered their filling at the oil-water interface (Dugyala, Muthukuru, Mani, & Basavaraj, 2016; Wang, Singh, & Behrens, 2012). To address this issue, some strategies have been applied for charge shielding, such as addition of electrolytes, surfactants, or protonation (Z. Hu, Ballinger, Pelton, & Cranston, 2015; Liu, et al., 2018; Pelegrini, et al., 2021). Concentrated hydrochloric acid and sodium hydroxide have been reported to remove the sulfate groups from the surface of CNCs, achieving desulfuration (Jiang, Esker, & Roman, 2010; Kalashnikova, Bizot, Cathala, & Capron, 2012; Kloser & Gray, 2010). However, complex operational processes and formulations not only increase costs, but also pose challenges to energy and environmental sustainability. Furthermore, CNC-stabilized Pickering emulsions exhibited low viscosity even in the presence of electrolytes, due to the weak interacting networks, which lead to more significant gravitational separation (Bai, et al., 2019). Recently, cellulose nanofibers (CNFs) have been employed to improve the performance of cellulose-based Pickering emulsions (Q. Li, et al., 2019; Wu, et al., 2020; Y. Wu, et al., 2021). The large axial dimensions and chain bendability allow CNF-stabilized Pickering emulsions to have complex fiber networks and excellent viscosity for emulsification and prevention of creaming (Goi, et al., 2019). However, CNFs typically require high energy emulsification equipment to form homogeneous emulsions, such as high pressure homogenizers, microfluidizers. The difference in surface chemistry likewise results in CNF-stabilized Pickering emulsions with high environmental sensitivity. For example, TEMPO-oxidized CNFs

were highly susceptible to electrolytes when used as emulsifiers, and simultaneously tended to form inhomogeneous oil droplets due to their high aspect ratio and charged surfaces that limited rapid adsorption at the oil-water interface (Aaen, Brodin, Simon, Heggset, & Syverud, 2019; Gestranius, Stenius, Kontturi, Sjöblom, & Tammelin, 2017). Despite surface modifications and additives have been widely used to adjust the surface activity or improve emulsifying stability of nanocellulose (Zhen Hu, Patten, Pelton, & Cranston, 2015; Y. Li, et al., 2018; Xu, Li, & Zhang, 2018), these strategies could not meet the requirements for emulsifiers in the fields of food, cosmetic, and pharmaceutical sectors. Therefore, it remains challenging to develop green, convenient, and stable nanocellulose-based Pickering emulsifiers.

Biological treatment is considered to be an appealing top-down strategy for the production of nanocellulose thanks to its high selectivity, green, sustainability, and mildness during enzymatic hydrolysis, which is largely compatible with the process design employed by modern lignocellulosic biorefineries (Peng, et al., 2022; Yarbrough, et al., 2017; Q. Zhang, et al., 2021; Zhu, Sabo, & Luo, 2011). The synergistic cleavage of β-1,4-glycoside bonds by cellulases facilitates the breakdown of cellulose to nanoscale, while simultaneously maximizing the preservation of amphiphilic properties of nanocellulose, rendering it an ideal candidate for food-grade emulsification purposes. Unfortunately, the utilization of enzymatically prepared nanocellulose in Pickering emulsions has been highly uncommon thus far.

Herein, we propose a green strategy to prepare nanocellulose *via* enzymatic hydrolysis for stabilizing Pickering emulsion. The effects of enzymatic hydrolysis on

the yield, morphology and chemical properties of ENC were investigated by controlling the digestion conditions. The emulsification mechanism of ENC was investigated by fluorescence staining and electron imaging. The morphology, emulsion index and rheological behavior of Pickering emulsion were systematically monitored. Furthermore, three ENC concentration-dependent Pickering emulsion phase behaviors were established by macro/micro-morphological differences. Importantly, tolerance of ENC-stabilized Pickering emulsion under harsh environments was also studied. This work provides a new green pathway for the development and application of nanocellulose-based Pickering emulsions in food, pharmaceutical and cosmetic sectors.

2. Experimental section

2.1. Materials

Pine pulp was obtained from State Key Laboratory of Pulp and Paper Engineering (Guangzhou, China). Styrene, soybean oil, paraffin liquid, dichloromethane, disodium hydrogen phosphate dodecahydrate, and cellulase from *Trichoderma viride* (enzyme activity is 15000 U/g) were purchased from Sinopharm Chemical Reagent Co., Ltd (Beijing, China). Calcofluor white was purchased from Sigma-Aldrich Trading Co., Ltd (Shanghai, China). Nile red, hexadecane, dodecane, citric acid monohydrate, and 2,2'-Azobis(2-methylpropionitrile) (AIBN) were purchased from Aladdin Reagent Co., Ltd (Shanghai, China). The above reagents were analytically pure and were used unpurified.

2.2. Enzymatic preparation of nanocellulose

The experiments for optimization of enzyme loading and hydrolysis time were performed in disodium hydrogen phosphate-citrate buffer (pH 5) at 50 °C. Briefly, pine

cellulose (dry weight: 0.50 g) was added into 50 mL solution and incubated with an enzyme loading of 100, 500, 1,000 and 5,000 U/g in Erlenmeyer flask (100 mL), respectively. Enzymatically prepared nanocellulose (ENC) was obtained by placing the mixture in an incubator shaker (THZ-103B, Yiheng Scientific Instruments, China). After reaction, each group of samples was placed in a boiling water bath for 20 mins to inactivate the enzymes. The supernatant was collected by filtration through a microporous membrane (Nylon 66, pore size: 0.2 μm), and the reducing sugar concentration was determined by the 3,5-dinitrosalicylic acid (DNS) method as previously described (Q. Zhang, et al., 2021). The solid residue was resuspended in deionized water and centrifuged at 12000 rpm (Sorvall ST16R, Thermo Fisher Scientific, USA) to remove the remaining buffer and enzyme. The precipitate was resuspended with deionized water and centrifuged the resulting mixture at 3000 rpm for 5 mins to collect the suspension. Finally, clear suspension was obtained by repeating above steps three times. The yields of ENC were determined by gravimetrical method after separating nanocellulose and unconverted bulk cellulose.

The collected ENC suspensions were concentrated by centrifugation to reach a concentration of 2.0 wt% and stored at 4 °C. ENC samples were named as ENC-12, ENC-24, and ENC-36, according to enzymatic times of 12, 24, and 36 h, respectively. The sulfuric acid hydrolyzed CNCs and the TEMPO-oxidized CNFs were prepared according to our previously reported methods (Huang, Yang, Yang, & Chang, 2021; Y. Zhang, Cheng, Chang, & Zhang, 2018).

2.3. Preparation of ENC-stabilized Pickering emulsions

Briefly, oil phase (1 mL) was vortex-mixed with ENC suspensions (9 g, 0.05-2.0 wt%) and then emulsified using the ultrasonic homogenizer (SCIENTZ-IID, Scientz Biotechnology, China) for 2 min in an ice bath at 200 W with alternating on-off cycles (2 ~ 3 s). The resultant emulsions were stored at room temperature for 14 days with continuous observation. Emulsions containing ENC (1.2 wt%) and various oil (10 wt%), such as hexadecane, dodecane, soybean oil, paraffin liquid, dichloromethane, and styrene, were prepared following the emulsification method described above.

2.4. Characterization

The structures of cellulose and nanocellulose were characterized by a NICOLET 5700 Fourier Transform infrared spectrometer (Thermo Fisher Scientific, USA). The morphology and size distribution of ENC were analyzed by a JEM-2100 transmission electron microscope (JEOL, Japan), where ENC suspensions (5 μL, 0.01 wt%) were dropped onto a copper grid and evaporated before measurement. The reducing sugar content of the filtrate was measured using double beam UV-visible spectrophotometer (MAPADA, China). The Zeta potential of ENC suspensions were measured using a Nanotrac Wave II analyzer (Microtrac, Germany). The O/W interfacial tension was measured by the pendant drop method using a LSA100 interfacial tensiometer (Lauda Scientific, Germany). Polarized optical microscopy (POM) measurements were carried out using an Axio Scope A1 polarizing microscope (Zeiss, Germany). The X-ray diffraction (XRD) patterns of the ENC were carried out on an XPert Pro XRD spectrometer (PANalytical, Netherlands). The crystallinity index (*CrI*) of the ENC was calculated according to a previous report (D. Huang, et al., 2021).

Scanning electron micrograph (SEM) images of polystyrene microspheres obtained by *in situ* polymerization of styrene/water emulsions were performed on a Zeiss SIGMA microscope (Zeiss, Germany) operated at 5 kV. The preparation of polystyrene microspheres was carried out according to the previously reported method (Kalashnikova, Bizot, Cathala, & Capron, 2011). The microstructure of emulsion was taken by DM28 fluorescence microscope (Leica, Germany), where the oil phase and ENC were stained with Nile red (1 mg mL^{-1} in ethanol) and Calcofluor white, respectively. Droplet size was counted by ImageJ software, based on diluted emulsion images obtained in the bright field. The emulsion index (*EI*) is calculated according to the following Eq. (1):

$$EI = \frac{H_c}{H_t} \times 100\% \quad (1)$$

where H_c is the height of the cream layer and H_t is the total height of the emulsion.

Rheological test of the ENC-stabilized Pickering emulsion was carried out on a Discovery HR-2 rheometer (TA Instruments, USA) with a 40 mm parallel plate at 25 °C, and the gap was set as 200 μm. The steady state shear viscosity of ENC suspensions and ENC-stabilized Pickering emulsions were monitored by increasing the shear rate from 0.01 to 100 s^{-1}. The strain sweep test was conducted for the linear viscoelastic region of ENC-stabilized Pickering emulsions by varying the strain from 0.1 to 100% at a constant frequency of 1 Hz. The frequency sweep test was measured under a constant strain of 1.0% to investigate the viscoelastic properties of Pickering emulsions with different ENC concentrations.

2.5. Stability of ENC-stabilized Pickering emulsions

The as-prepared emulsions (0.8 wt% ENC and 10 wt% hexadecane) were immediately placed at 4, 25, 37, and 70 °C for 7 days, respectively, to evaluate the effects of temperature on the stability of emulsions. On contrary, ENC-stabilized Pickering emulsions with different NaCl concentrations (0, 0.5, 1.0, 1.5, and 2.0 M) and pH values (1, 4, 7, 10, and 13) were also prepared and stored at room temperature for 7 days. The morphology and property of emulsions were recorded as previously described. To investigate the effect of centrifugation, Nile red stained emulsion (1 mL) was centrifuged at 10000 rpm for 10 min (H1650R, Cence, China). Fluorescent images of emulsions were recorded before and after the centrifugation. The samples were resuspended using a vortex oscillator and the optical microscopic morphology of the resuspended emulsions were observed.

3. Results and discussion

3.1 Preparation of ENC

Generally, cellulose consists of crystalline regions with highly ordered cellulose chains and amorphous regions with disordered cellulose chains. Compared to crystalline regions, the amorphous regions of cellulose are preferentially hydrolyzed by enzymes in aqueous media, which provides an opportunity to obtain nanocellulose (Chen, Pang, Shen, Tong, & Jia, 2019). As shown in **Fig. 1a**, anchoring of enzyme molecules on the substrate surface promoted the degradation of cellulose chains, where endoglucanase (EG) randomly hydrolyzed the β-1,4-glycoside bonds within the amorphous region to produce new chain ends, and cellobiohydrolase (CBH) acted on the amorphous or crystalline regions to release cellobiose mainly from the ends of

cellulose chains (Brunecky, et al., 2013; Yarbrough, et al., 2017). The β-glucosidases (BG) did not act on cellulose itself but broke cellobiose down to glucose. In this case, a positive disintegration of the cellulose substrate occurred under the synergistic action of multiple enzymes. The yield of ENC directly depended on enzyme loadings, as shown in **Fig. S1a**. As the enzyme loadings raised from 100 U/g to 1000 U/g, nanocellulose yield increased from 8.2% to 34.7%, respectively, whereas the unconverted cellulose decreased from 83.3% to 34.4%, respectively, revealing that nanocellulose was isolated from bulk cellulose by enzymatic hydrolysis. After enzyme loadings reached 5000 U/g, the yield of the ENC decreased to 27.9%, but soluble sugars yield further increased to 39.1% (**Fig. S1b**), indicating that exfoliated nanocellulose was further degraded into soluble sugars by excessive cellulase. Therefore, an enzyme loading of 1000 U/g was selected for the preparation of ENC to avoid excessive hydrolysis of nanocellulose.

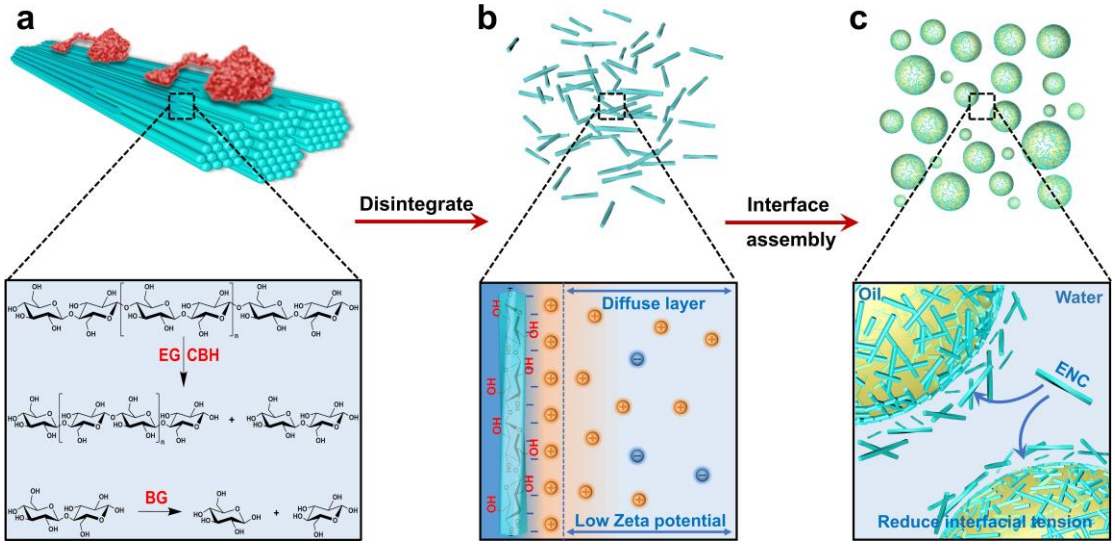

Fig. 1. Schematic diagram of enzymatic preparation and surface properties of ENC. (a) The active disintegration of cellulose substrate under the synergistic action of multiple

enzymes. (b) The formation of electrical double layer in ENC suspensions. (c) The assembly of ENC at the oil/water interface.

In the early stage of enzymatic hydrolysis, bulk cellulose disintegrated into inhomogeneous fragments through the random degradation of the amorphous regions (**Fig. S2**). With the extension of enzymatic hydrolysis time, CBH promoted the unidirectional hydrolysis of cellulose, allowing further degradation of the small fragments. The highest yield (32.9%) of ENC was achieved after enzymolysis for 24 h, while the excessive hydrolysis at 36 h led to a significant decrease (24.3%) in the yield of nanocellulose (**Fig. S3**). The morphology and size of ENC were directly relevant to the degree of enzymatic digestion (**Fig. S4a**). As the enzymolysis time increased from 12 to 36 h, the size distribution of ENC became more uniform, where the average diameter and the length of ENC decreased sharply from 41.3 to 22.7 nm and 1437.6 to 426.8 nm, respectively (**Fig. S4b**). Compared to the native cellulose, the chemical structure and cellulose I crystals of ENC changed hardly, but the *CrI* of ENC increased slightly to 75% due to enzymolysis of cellulose amorphous regions (**Fig. S5**).

Typically, the hydrophilic and hydrophobic planes of cellulose I crystals provide amphiphilic character to nanocellulose, but the long-range electrostatic repulsion controlled by surface charged groups severely hinders the interfacial assembly of colloidal particles (Capron, Rojas, & Bordes, 2017; Maeda & Maeda, 2015). Fortunately, the enzymatic preparation of nanocellulose well preserved the surface chemical properties of cellulose. The natural polar hydroxyl groups on the surface of

ENC created a small potential difference between the diffuse layer and adsorption layer, resulting in a low Zeta potential (**Fig. 1b**). Despite ENC-36 showed the higheset Zeta potential (-21.5 mV) among ENC samples, it was still lower than that of CNCs (-41.9 mV) prepared by sulfuric acid and CNFs (-35.4 mV) prepared by TEMPO oxidation (**Fig. S6a**). These results indicated that the charged sulfate groups or carboxyl groups greatly expanded the thickness of the electrical double layer of nanocellulose in the suspension(**Fig. S6b**). The dynamic interfacial tension of ENC on the oil/water interface was also lower than that of CNCs or CNFs (**Fig. S7**). The assembly of ENC with low surface potential at the oil-water interface promoted the reduction of interfacial tension (**Fig. 1c**), which would benefit their application as emulsifier for Pickering emulsions. In addition, the interfacial tension of ENC-24 on the oil/water interface was similar to that of ENC-36. Considering that the yield of ENC-24 was higher than ENC-36, ENC-24 was selected as the emulsifier for Pickering emulsions.

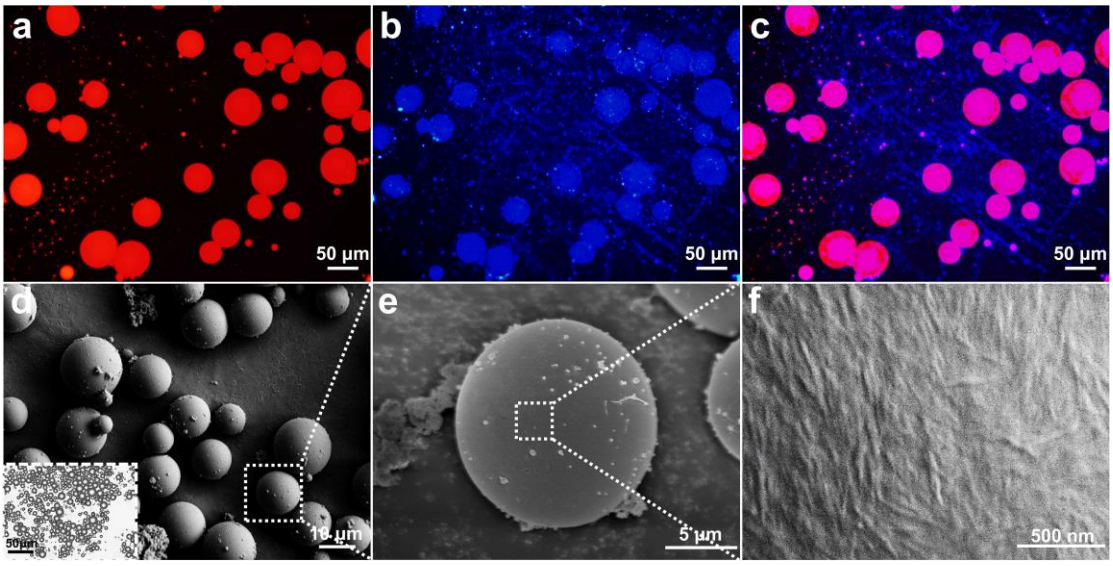

Fig. 2. The distribution of ENC at the oil-water interface. (a-c) Fluorescent micrographs of ENC-stabilized Pickering emulsions: Nile red stained oil droplets (a), Calcofluor

white stained ENC (b), and merged images (c). (d-f) SEM images of styrene-water emulsion stabilized by ENC after *in situ* polymerization under different magnifications.

3.2 Emulsification characteristics of ENC

Due to differences in the aggregation forms of colloidal particles at multiphase interfaces, biphasic fluorescent staining and *in situ* polymerization were employed to investigate the distribution of ENC in oil-water interface. The spherical oil droplets could be observed in the suspension after hexadecane were stained by Nile red (**Fig. 2a**). This result revealed that stable oil/water emulsions could be prepared by using ENC as emulsifiers. After stained by calcofluor white, ENC with blue fluorescence in the emulsion could be clearly distinguished (**Fig. 2b**). Most ENC distributed on the surface of oil droplets, and spherical profile appeared in the merged fluorescence image (**Fig. 2c**), confirming that ENC stabilized the emulsion in the form of interfacial adsorption. To further estimate the morphology of ENC at oil/water interface, *in situ* polymerization of styrene monomers was conducted in ENC-stabilized styrene/water emulsions by using AIBN as an initiator (**Fig. 2d**). ENC-coated monodispersed microspheres were obtained, which exhibited smooth surface (**Fig. 2e**). The spindle shaped ENC randomly distributed on the surface of polystyrene microspheres could be observed under high magnification (**Fig. 2f**). These results suggested that ENC adsorbed and assembled at the oil/water interface to stabilize Pickering emulsions, due to its short length and low surface potential.

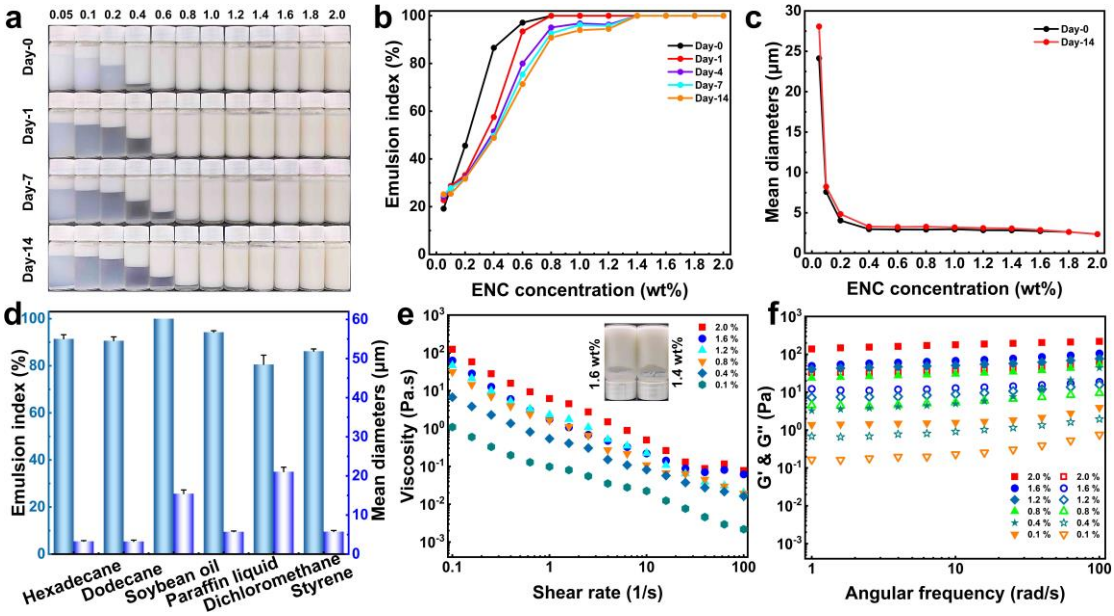

Fig. 3. The characterization of ENC-stabilized Pickering emulsions. (a) Visual appearance, (b) emulsion index, and (c) oil droplets diameter of Pickering emulsions stabilized by ENC with different concentrations. (d) The emulsion index and oil droplets diameter of Pickering emulsions containing different oil phases. (e) Viscosity and (f) viscoelasticity curves of Pickering emulsions with different ENC concentrations.

The stability of Pickering emulsions was influenced by ENC concentrations, as shown in **Fig. 3a**. ENC as low as 0.05 wt% could successfully form an emulsion without oil droplet leakage, but significant creaming occurred because of the difference in the density between oil and water phases. As the ENC concentrations gradually increased, the cream layer in the emulsions thickened rapidly, where a uniform emulsion was obtained after the ENC concentration reached to 1.4 wt%, indicating that ENC effectively prevented the occurrence of creaming behavior. **Fig. 3b** specifically shows

306 the variation of the emulsion index with the ENC concentrations and storage days. The
307 low surface potential of ENC not only promoted the interfacial adsorption behavior, but
308 also enhanced their van der Waals forces and hydrogen bonding interactions within the
309 continuous phase. Therefore, the rapid increase of the emulsion index in concentration
310 range of 0.05 wt% to 0.8 wt% was mainly attributed to the formation of ENC networks
311 within continuous phase. As the ENC concentration reached to 1.4 wt%, the continuous
312 ENC networks completely formed, and the creaming of emulsion was greatly inhibited.
313 In addition, the reduction in oil droplet size facilitates overcoming the occurrences
314 of creaming aggravated by gravitational factors (Bai, et al., 2019). The average
315 diameter of oil droplets decreased dramatically as ENC concentration increased from
316 0.05 to 0.4 wt%, but changed slightly after further increasing the ENC concentrations
317 (**Fig. 3c**). During emulsification, oil phase was converted into droplets by continuous
318 shearing. When ENC in the emulsion was not enough to stabilize large specific surface
319 area of oil phase, large droplets generated to reduce the total interfacial area of the
320 system (**Fig. S8**). Taking the advantage of their low surface potential and fast interfacial
321 adsorption rate (Bertsch, et al., 2020; Pandey, et al., 2018), ENC could keep the
322 diameter of oil droplets below 30 μm, even when the concentration was as low as 0.05
323 wt%. As the ENC concentration reached a critical value (i.e., 0.4 wt%), the total
324 interfacial area could be stabilized by enough ENC, resulting in the formation of
325 uniform oil droplets. At this point, the diameters of oil droplets were mainly dominated
326 by shearing force and the size of ENC. Remarkably, the diameter of oil droplets almost
327 did not change with the increase of storage days (**Fig. S9**). Compared to CNCs and

CNFs (Gestranius, et al., 2017; Yuan, Zeng, Wang, Cheng, & Chen, 2021), ENC could better control the shape, size, and surface properties of oil droplets, thus forming stable emulsions (**Fig. S10**). For various oils (hexadecane, dodecane, soybean oil, paraffin liquid, dichloromethane, and styrene), the emulsion index and oil droplet diameter (less than 30 μm) were ranged from 80.6% to 100% and from 3.2 μm to 21 μm, respectively (**Fig. 3d**), demonstrating the universal applicability and controllability of ENC as green colloidal emulsifiers.

Fig. 3e shows the shear thinning behavior of ENC-stabilized Pickering emulsions. The viscosity of Pickering emulsions exhibited an order of magnitude growth with increasing ENC concentrations, and self-supporting Pickering emulsions could be obtained when the ENC concentration reached 1.4 wt%. The storage modulus (G') of emulsions were consistently higher than the loss modulus (G'') and independent with the oscillation frequency, further illustrating the gel-like behavior of the ENC-stabilized Pickering emulsions (**Fig. 3f**). Normally, the electrostatic repulsion of charged groups on the surface of nanocellulose reduces the viscosity and the dynamic modulus of nanocellulose suspensions (M. C. Li, Wu, Moon, Hubbe, & Bortner, 2021), however, the low surface potential of ENC enables van der Waals forces and hydrogen bonding to be the dominant particle-particle interactions, which confers excellent viscoelasticity to ENC-stabilized Pickering emulsions. In addition, the viscosity of Pickering emulsions increased significantly compared to the ENC suspensions (**Fig. S11**), suggesting that ENC-stabilized Pickering emulsions not only had particle-particle

interactions, but also encompassed strong interface-particle interactions, which were controlled by the interfacial assembly behavior of ENC.

To examine the effects of ENC concentration on phase behavior of emulsions, the fluorescence images of various Pickering emulsions are shown in **Fig. S12**. Monodisperse oil droplets could be observed in emulsions when the concentrations of ENC were 0.05 and 0.1 wt%. As the ENC concentration increased to 0.2 wt%, the flocculation of oil droplets appeared and gradually enhanced until large oil droplet clusters could be clearly observed at 1.2 wt%. Conversely, the oil droplet aggregates became significantly smaller and flocculation was remarkably reduced, as the ENC concentration reached to 1.4 wt%. According to above results, the concentration-dependent phase behavior of ENC-stabilized Pickering emulsions were divided into three stages, which were monodisperse droplets at low concentrations (i.e., 0.05-0.1 wt%), flocculation of droplets at medium concentrations (i.e., 0.2-1.2 wt%), and droplets dispersed in continuous networks at high concentrations (i.e., 1.4-2.0 wt%). The phase behaviors are closely related to the appearance and micromorphology of Pickering emulsions. At low ENC concentrations, a unique double-layer structure could be observed, where the cream layer consisted of large monodisperse oil droplets and the lower layer consisted of small ones (**Fig. 4a**). When the ENC reached medium concentrations, oil droplet clusters formed in the cream layer of the emulsions, while the number of oil droplets in the lower layer was greatly reduced, producing a relatively clear aqueous phase (**Fig. 4b**). For high ENC concentrations, emulsion samples with no

creaming were obtained, where reduced large clusters and relatively well dispersed oil droplets could be observed simultaneously in the top and bottom layers (**Fig. 4c**).

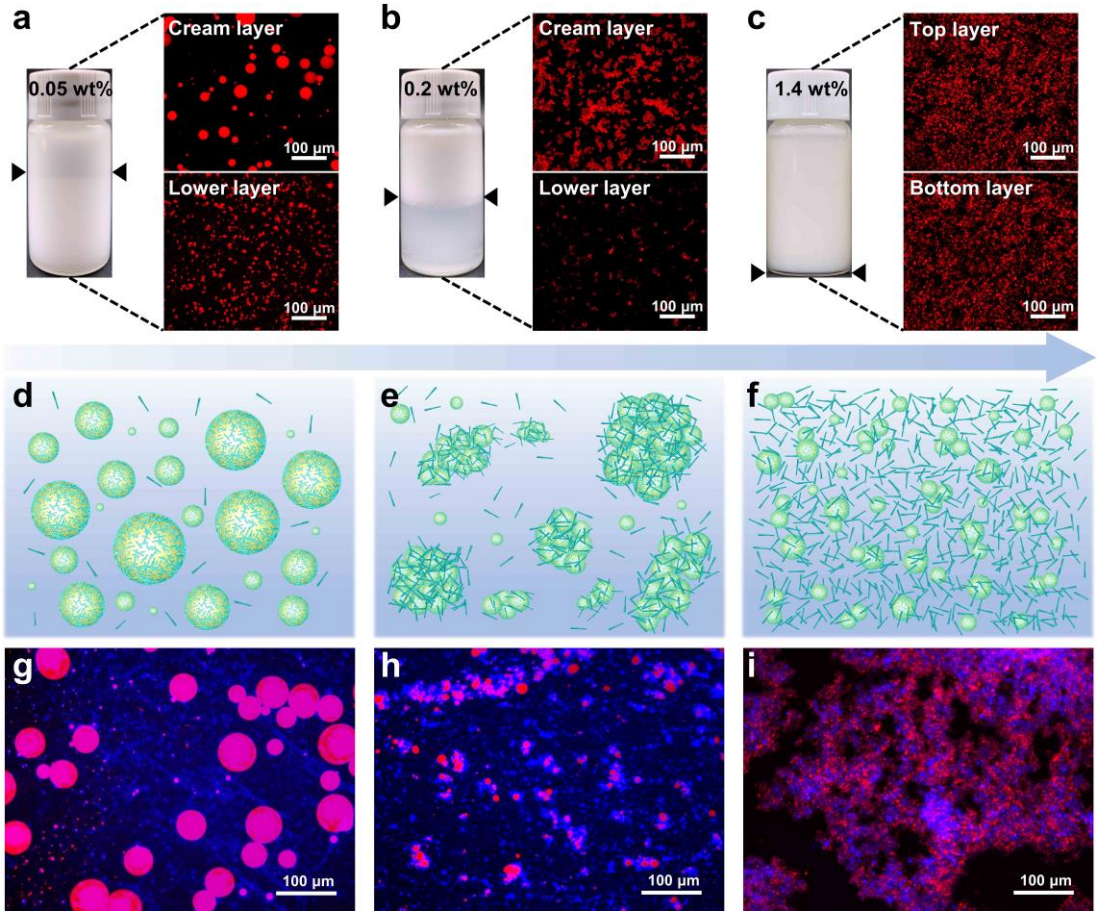

Fig. 4. Phase behavior of ENC-stabilized Pickering emulsions. (a-c) Visual appearance and microscopic morphology of the upper and lower layers of Pickering emulsion stabilized by different concentrations. (d-f) Schematic diagrams of the concentration-dependent phase behavior of ENC-stabilized Pickering emulsions. (g-i) Biphasic fluorescence staining of three concentrations (i.e., 0.05, 0.2, 1.4 wt%) of ENC-stabilized Pickering emulsion.

The schematic diagrams of the concentration-dependent phase behavior of ENC-stabilized Pickering emulsions are displayed in **Fig. 4d-f**. At low concentrations (i.e.,

382 0.05-0.1 wt%), monodispersed oil droplets were established because ENC were mainly
383 adsorbed at the oil-water interface, resulting in a weak interaction between oil droplets
384 (**Fig. 4d**). This speculation could be confirmed by biphasic fluorescence staining of
385 ENC-stabilized Pickering emulsion, as shown in **Fig. 4g**. Under the competition
386 between Brownian motion and gravitational field, large oil droplets quickly floated up
387 forming the cream layer, while small ones suspended in the lower layer. With increasing
388 storage days, small oil droplets gradually floated up, resulting in a thicker cream layer
389 and an increased emulsion index (**Fig. S13**). At the medium ENC concentrations (i.e.,
390 0.2-1.2 wt%), the flocculation phenomenon could be attributed to the bridging or
391 wrapping effect of ENC aggregates on oil droplets (**Fig. 4e**). ENC with a low surface
392 potential did not create a strong electrostatic barrier at the oil-water interface. Therefore,
393 the van der Waals forces and hydrogen bonding interactions promoted further
394 aggregation of the ENC on the surface of oil droplets as the ENC concentrations
395 increased within the continuous phase (**Fig. 4h**), which contributed to the occurrence
396 of flocculation. After storing for 14 days, water in the cream layer was further excluded,
397 leading to the decrease of emulsion index (**Fig. S13**). In addition, Pickering emulsions
398 containing different types of oils were applied for a comparative study of the phase
399 behavior (**Fig. S14**). The oil droplet clusters were found in various emulsions, further
400 indicating that the flocculation of emulsions was induced by medium ENC
401 concentrations. For high ENC concentrations (i.e., 1.4-2.0 wt%), a continuous network
402 completely formed by the excess ENC in the aqueous phase through van der Waals
403 forces and hydrogen bonding interactions that enabled the oil droplets to be uniformly

trapped (**Fig. 4f**). The relative position of oil droplets and ENC could be distinguished after staining, confirming the ability of ENC to capture oil droplets (**Fig. 4i**). Notably, unlike entangled network formed directly by CNFs, the network structure of ENC-stabilized Pickering emulsions is mainly attributed to strong particle-particle and interface-particle interactions dominated by proximity interaction forces.

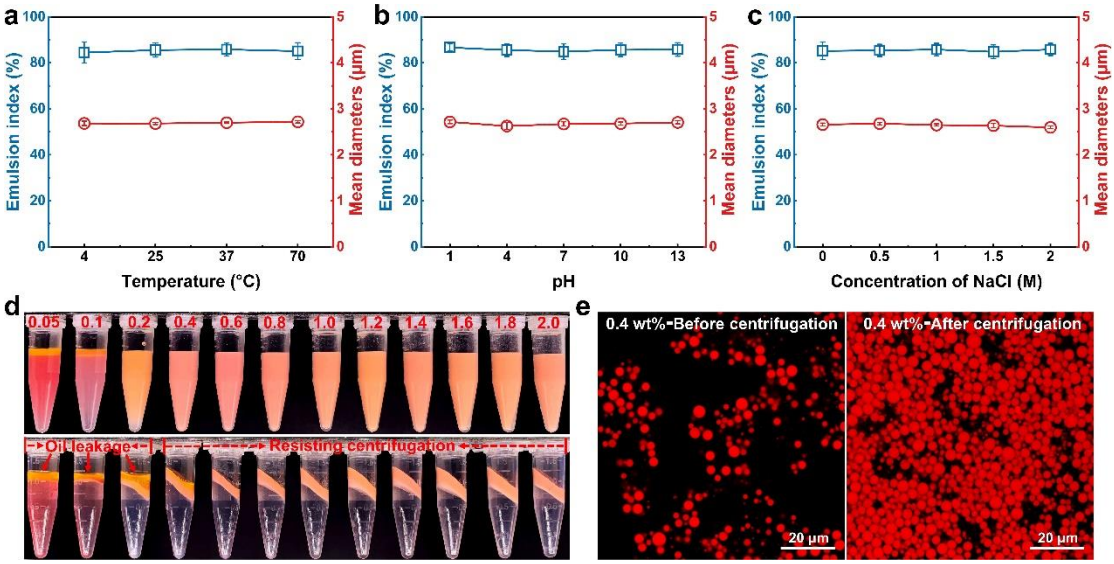

Fig. 5. Stability of ENC-stabilized Pickering emulsions. (a-c) Emulsion index and oil droplet diameters of ENC-stabilized Pickering emulsions at different temperature (a), pH values (b), and NaCl concentration (c). (d) Visual appearance of various Pickering emulsions before and after the centrifugation. (e) Fluorescence microscopy images of ENC-stabilized Pickering emulsion (0.4 wt%) before and after the centrifugation.

3.3. Stability of ENC-stabilized Pickering emulsions

Compared to traditional surfactants, particle emulsifiers had irreversible interfacial adsorption and higher interfacial desorption energy, which were conducive to the inhibition of emulsion instability (Bizmark & Ioannidis, 2017). The external

environment also affects the stability of the emulsions. Medium concentrations of ENC-stabilized Pickering emulsions were adopted to investigate the effects of temperature, salt concentration, pH, and centrifugation on the stability of the emulsions. The consistency of the appearance and oil droplet morphology of each emulsion were observed at external temperature range of 4 °C to 70 °C (**Fig. S15**). The size of oil droplets and emulsion index of emulsions changed slightly as the change of temperature (**Fig. 5a**). Although the enthalpy increase of the system at high temperatures would promote the desorption behavior of colloidal particles at the oil-water interface, the ENC-stabilized Pickering emulsions still exhibited excellent temperature resistance, which could be attributed to the strong interfacial adsorption layer and interaction network formed by ENC. On contrary, the electrolytes have a great influence on the stability of colloidal dispersions according to the DLVO theory (Hotze, Phenrat, & Lowry, 2010). Owing to the competition between the electrostatic repulsion and the van der Waals force, the charged groups on the colloidal surface are sensitive to the electrolytes in the system. For ENC-stabilized Pickering emulsions, the appearance and oil droplet morphology changed hardly at different pH values (**Fig. S16**) or NaCl concentrations (**Fig. S17**). As the pH values increased from 1 to 13, the emulsion index and the mean diameter of oil droplets maintained at approximately 85% and 2.7 μm, respectively (**Fig. 5b**). Similarly, the oil droplet diameter and emulsion index also did not undergo large fluctuations, when the concentration of NaCl increased from 0 to 2 M (**Fig. 5c**). These results could be attributed to the intermolecular forces that

dominated by van der Waals forces and hydrogen bonds, which conferred the insensitivity of ENC-stabilized Pickering emulsions to electrolytes.

The stability of emulsions with different ENC concentrations under centrifugal treatment was also investigated, as shown in **Fig. 5d**. After a high-speed centrifugation (10000 rpm), water was excluded out from the emulsions and a cream layer with high concentrated oil droplets was formed. At low ENC concentrations (< 0.2 wt%), oil leakage occurred and clear orange oil layer could be observed, which was attributed to the collapse of the adsorption layer under centrifugal force. However, as ENC concentrations reached 0.4 wt%, oil droplets were firmly locked in a homogeneous cream layer after the centrifugation. The highly concentrated oil droplets could be observed in the fluorescence microscopy image after the centrifugation, but no oil droplet coalescence occurred (**Fig. 5e**). Furthermore, after resuspension of the centrifuged emulsion samples, the morphology of oil droplets remained highly consistent with that before the centrifugation (**Fig. S18**). These results indicated that the solid interfacial adsorption layer formed by ENC conferred excellent concentration and redispersion properties to the emulsion.

4. Conclusions

We have demonstrated the preparation of nanocellulose by enzymatic hydrolysis for stabilizing Pickering emulsions. Compared to traditional surface charged nanocellulose, ENC inherently had lower Zeta potential and oil/water interfacial tension, facilitating the formation of stable Pickering emulsions. The short axial dimension and the low surface potential of ENC enabled them to assemble a dense

adsorption layer at the oil-water interface, which could effectively control the size and morphology of oil droplets in the emulsion. The van der Waals forces and hydrogen bonding interactions were maximized because of the absence of charged groups on the surface of ENC, giving them strong particle-particle and interface-particle interactions to enhance the viscoelasticity of Pickering emulsion. The concentration-dependent phase behaviors of ENC-stabilized Pickering emulsions could be divided into three regions: (i) monodisperse droplets at low concentrations, (ii) flocculation of droplets at medium concentrations, and (iii) droplets dispersed in continuous networks at high concentrations. Furthermore, ENC-stabilized Pickering emulsions exhibited excellent stability under different external environments (e.g., temperature, pH, NaCl concentration and centrifugation). This work provides a green strategy to prepare nanocellulose *via* enzymatic hydrolysis for stabilizing Pickering emulsions.

Author information

Corresponding author

E-mail: changcy@whu.edu.cn (C. Chang)

wangzaigui2013@163.com (Z. Wang)

Notes

The authors declare no competing financial interest.

Acknowledgements

This work was financially supported by the National Natural Science Foundation of

China (52073217, 51873164), the National Key Research and Development Program of China (2018YFE0123700), and Key Research and Development Program of Hubei Province (2020BCA079).

References

Aaen, R., Brodin, F. W., Simon, S., Heggset, E. B., & Syverud, K. (2019). Oil-in-water emulsions stabilized by cellulose nanofibrils-The effects of ionic strength and pH. *Nanomaterials, 9*(2), 259.

Albert, C., Beladjine, M., Tsapis, N., Fattal, E., Agnely, F., & Huang, N. (2019). Pickering emulsions: Preparation processes, key parameters governing their properties and potential for pharmaceutical applications. *Journal of Controlled Release, 309*, 302-332.

Bai, L., Lv, S., Xiang, W., Huan, S., McClements, D. J., & Rojas, O. J. (2019). Oil-in-water Pickering emulsions via microfluidization with cellulose nanocrystals: 1. Formation and stability. *Food Hydrocolloids, 96*, 699-708.

Bertsch, P., & Fischer, P. (2020). Adsorption and interfacial structure of nanocelluloses at fluid interfaces. *Advances in Colloid and Interface Science, 276*, 102089.

Binks, B. P., Philip, J., & Rodrigues, J. A. (2005). Inversion of silica-stabilized emulsions induced by particle concentration. *Langmuir, 21*(8), 3296-3302.

Bizmark, N., & Ioannidis, M. A. (2017). Ethyl cellulose nanoparticles at the alkane-water interface and the making of Pickering emulsions. *Langmuir, 33*(40), 10568-10576.

Brunecky, R., Alahuhta, M., Xu, Q., Donohoe, B. S., Crowley, M. F., Kataeva, I. A., Yang, S. J., Resch, M. G., Adams, M. W. W., Lunin, V. V., Himmel, M. E., & Bomble, Y. J. (2013). Revealing nature's cellulase diversity: The digestion mechanism of *Caldicellulosiruptor bescii* CelA. *Science, 342*(6165), 1513-1516.

Brunier, B., Sheibat-Othman, N., Chniguir, M., Chevalier, Y., & Bourgeat-Lami, E. (2016). Investigation of four different laponite clays as stabilizers in Pickering emulsion polymerization. *Langmuir, 32*(24), 6046-6057.

Capron, I., Rojas, O. J., & Bordes, R. (2017). Behavior of nanocelluloses at interfaces. *Current Opinion in Colloid & Interface Science, 29*, 83-95.

Chen, X.-Q., Pang, G.-X., Shen, W.-H., Tong, X., & Jia, M.-Y. (2019). Preparation and characterization of the ribbon-like cellulose nanocrystals by the cellulase enzymolysis of cotton pulp fibers. *Carbohydrate Polymers, 207*, 713-719.

Cui, Z. G., Shi, K. Z., Cui, Y. Z., & Binks, B. P. (2008). Double phase inversion of emulsions stabilized by a mixture of CaCO3 nanoparticles and sodium dodecyl sulphate. *Colloids and Surfaces a-Physicochemical and Engineering Aspects, 329*(1-2), 67-74.

Dugyala, V. R., Muthukuru, J. S., Mani, E., & Basavaraj, M. G. (2016). Role of electrostatic interactions in the adsorption kinetics of nanoparticles at fluid-fluid interfaces. *Physical Chemistry Chemical Physics, 18*(7), 5499-5508.

Gestranius, M., Stenius, P., Kontturi, E., Sjöblom, J., & Tammelin, T. (2017). Phase behaviour and droplet size of oil-in-water Pickering emulsions stabilised with

plant-derived nanocellulosic materials. *Colloids and Surfaces A: Physicochemical and Engineering Aspects, 519*, 60-70.

Goi, Y., Fujisawa, S., Saito, T., Yamane, K., Kuroda, K., & Isogai, A. (2019). Dual functions of TEMPO-oxidized cellulose nanofibers in oil-in-water emulsions: A Pickering emulsifier and a unique dispersion stabilizer. *Langmuir, 35*(33), 10920-10926.

Guo, J. X., Cui, L. J., & Meng, Z. (2023). Oleogels/emulsion gels as novel saturated fat replacers in meat products: A review. *Food Hydrocolloids, 137*, 108313.

Hotze, E. M., Phenrat, T., & Lowry, G. V. (2010). Nanoparticle aggregation: Challenges to understanding transport and reactivity in the environment. *Journal of Environmental Quality, 39*(6), 1909-1924.

Hu, Z., Ballinger, S., Pelton, R., & Cranston, E. D. (2015). Surfactant-enhanced cellulose nanocrystal Pickering emulsions. *Journal of Colloid and Interface Science, 439*, 139-148.

Hu, Z., Patten, T., Pelton, R., & Cranston, E. D. (2015). Synergistic stabilization of emulsions and emulsion gels with water-soluble polymers and cellulose nanocrystals. *ACS Sustainable Chemistry & Engineering, 3*(5), 1023-1031.

Huang, D., Li, D., Mo, K., Xu, R., Huang, Y., Cui, Y., Zhang, Q., & Chang, C. (2021). Top-down fabrication of biodegradable multilayer tunicate cellulose films with controlled mechanical properties. *Cellulose, 28*(16), 10415-10424.

548 Huang, Y., Yang, P., Yang, F., & Chang, C. (2021). Self-supported nanoporous
549 lysozyme/nanocellulose membranes for multifunctional wastewater purification.
550 *Journal of Membrane Science, 635*, 119537.
551 Jiang, F., Esker, A. R., & Roman, M. (2010). Acid-catalyzed and solvolytic desulfation
552 of H_2SO_4-hydrolyzed cellulose nanocrystals. *Langmuir, 26*(23), 17919-17925.
553 Jiao, B., Shi, A., Wang, Q., & Binks, B. P. (2018). High-internal-phase Pickering
554 emulsions stabilized solely by peanut-protein-isolate microgel particles with
555 multiple potential applications. *Angewandte Chemie-International Edition, 57*(30),
556 9274-9278.
557 Kalashnikova, I., Bizot, H., Cathala, B., & Capron, I. (2011). New Pickering emulsions
558 stabilized by bacterial cellulose nanocrystals. *Langmuir, 27*(12), 7471-7479.
559 Kalashnikova, I., Bizot, H., Cathala, B., & Capron, I. (2012). Modulation of cellulose
560 nanocrystals amphiphilic properties to stabilize oil/water interface.
561 *Biomacromolecules, 13*(1), 267-275.
562 Kedzior, S. A., Gabriel, V. A., Dube, M. A., & Cranston, E. D. (2021). Nanocellulose
563 in emulsions and heterogeneous water-based polymer systems: A review.
564 *Advanced Materials, 33*(28), e2002404.
565 Kloser, E., & Gray, D. G. (2010). Surface grafting of cellulose nanocrystals with
566 poly(ethylene oxide) in aqueous media. *Langmuir, 26*(16), 13450-13456.
567 Laredj-Bourezg, F., Bolzinger, M.-A., Pelletier, J., & Chevalier, Y. (2017). Pickering
568 emulsions stabilized by biodegradable block copolymer micelles for controlled
569 topical drug delivery. *International Journal of Pharmaceutics, 531*(1), 134-142.

570 Li, M. C., Wu, Q., Moon, R. J., Hubbe, M. A., & Bortner, M. J. (2021). Rheological
571 aspects of cellulose nanomaterials: Governing factors and emerging applications.
572 *Advanced Materials, 33*(21), e2006052.
573 Li, Q., Wang, Y., Wu, Y., He, K., Li, Y., Luo, X., Li, B., Wang, C., & Liu, S. (2019).
574 Flexible cellulose nanofibrils as novel pickering stabilizers: The emulsifying
575 property and packing behavior. *Food Hydrocolloids, 88*, 180-189.
576 Li, Q., Wu, Y., Fang, R., Lei, C., Li, Y., Li, B., Pei, Y., Luo, X., & ShilinLiu. (2021).
577 Application of nanocellulose as particle stabilizer in food Pickering emulsion:
578 Scope, merits and challenges. *Trends in Food Science & Technology, 110*, 573-583.
579 Li, Y., Liu, X., Zhang, Z., Zhao, S., Tian, G., Zheng, J., Wang, D., Shi, S., & Russell, T.
580 P. (2018). Adaptive structured Pickering emulsions and porous materials based on
581 cellulose nanocrystal surfactants. *Angewandte Chemie-International Edition,*
582 *57*(41), 13560-13564.
583 Liu, L., Hu, Z., Sui, X., Guo, J., Cranston, E. D., & Mao, Z. (2018). Effect of counterion
584 choice on the stability of cellulose nanocrystal Pickering emulsions. *Industrial &*
585 *Engineering Chemistry Research, 57*(21), 7169-7180.
586 Low, L. E., Siva, S. P., Ho, Y. K., Chan, E. S., & Tey, B. T. (2020). Recent advances of
587 characterization techniques for the formation, physical properties and stability of
588 Pickering emulsion. *Advances in Colloid and Interface Science, 277*, 102117.
589 Maeda, H., & Maeda, Y. (2015). Orientation-dependent London-van der Waals
590 interaction energy between macroscopic bodies. *Langmuir, 31*(26), 7251-7263.

Ni, L., Yu, C., Wei, Q., Liu, D., & Qiu, J. (2022). Pickering emulsion catalysis: Interfacial chemistry, catalyst design, challenges, and perspectives. *Angewandte Chemie-International Edition, 61*(30), e202115885.

Pandey, A., Derakhshandeh, M., Kedzior, S. A., Pilapil, B., Shomrat, N., Segal-Peretz, T., Bryant, S. L., & Trifkovic, M. (2018). Role of interparticle interactions on microstructural and rheological properties of cellulose nanocrystal stabilized emulsions. *Journal of Colloid and Interface Science, 532*, 808-818.

Parajuli, S., & Urena-Benavides, E. E. (2022). Fundamental aspects of nanocellulose stabilized Pickering emulsions and foams. *Advances in Colloid and Interface Science, 299*, 102530.

Pelegrini, B. L., Fernandes, F. M. B., Fernandes, T., de Oliveira, J. H., Rosseto, H. C., Junior, A. G. O., Reis, A. V., Castelani, E. V., Sobral, F. N. C., Shirabayashi, W. V. I., Benyahia, L., Chassenieux, C., & de Souza Lima, M. M. (2021). Novel green strategy to improve the hydrophobicity of cellulose nanocrystals and the interfacial elasticity of Pickering emulsions. *Cellulose, 28*(10), 6201-6238.

Peng, H., Zhao, W., Liu, J., Liu, P., Yu, H., Deng, J., Yang, Q., Zhang, R., Hu, Z., Liu, S., Sun, D., Peng, L., & Wang, Y. (2022). Distinct cellulose nanofibrils generated for improved Pickering emulsions and lignocellulose-degradation enzyme secretion coupled with high bioethanol production in natural rice mutants. *Green Chemistry, 24*(7), 2975-2987.

611 Perrin, L., Gillet, G., Gressin, L., & Desobry, S. (2020). Interest of Pickering emulsions
612 for sustainable micro/nanocellulose in food and cosmetic applications. *Polymers, 12*(10), 2385.
613
614 Wang, H. Z., Singh, V., & Behrens, S. H. (2012). Image charge effects on the formation
615 of Pickering emulsions. *Journal of Physical Chemistry Letters, 3*(20), 2986-2990.
616 Wu, B., Yang, C., Xin, Q., Kong, L., Eggersdorfer, M., Ruan, J., Zhao, P., Shan, J., Liu,
617 K., Chen, D., Weitz, D. A., & Gao, X. (2021). Attractive Pickering emulsion gels.
618 *Advanced Materials, 33*(33), e2102362.
619 Wu, J., Zhu, W., Shi, X., Li, Q., Huang, C., Tian, Y., & Wang, S. (2020). Acid-free
620 preparation and characterization of kelp (Laminaria japonica) nanocelluloses and
621 their application in Pickering emulsions. *Carbohydrate Polymers, 236*, 115999.
622 Wu, Y., Zhang, X., Qiu, D., Pei, Y., Li, Y., Li, B., & Liu, S. (2021). Effect of surface
623 charge density of bacterial cellulose nanofibrils on the rheology property of O/W
624 Pickering emulsions. *Food Hydrocolloids, 120*, 106944.
625 Xu, H. N., Li, Y. H., & Zhang, L. (2018). Driving forces for accumulation of cellulose
626 nanofibrils at the oil/water interface. *Langmuir, 34*(36), 10757-10763.
627 Yarbrough, J. M., Zhang, R., Mittal, A., Vander Wall, T., Bomble, Y. J., Decker, S. R.,
628 Himmel, M. E., & Ciesielski, P. N. (2017). Multifunctional cellulolytic enzymes
629 outperform processive fungal cellulases for coproduction of nanocellulose and
630 biofuels. *ACS Nano, 11*(3), 3101-3109.

631 Yuan, T., Zeng, J., Wang, B., Cheng, Z., & Chen, K. (2021). Pickering emulsion
632 stabilized by cellulosic fibers: Morphological properties-interfacial stabilization-
633 rheological behavior relationships. *Carbohydrate Polymers, 269*, 118339.
634 Zhang, Q., Lu, Z., Su, C., Feng, Z., Wang, H., Yu, J., & Su, W. (2021). High yielding,
635 one-step mechano-enzymatic hydrolysis of cellulose to cellulose nanocrystals
636 without bulk solvent. *Bioresource Technology, 331*, 125015.
637 Zhang, Y., Cheng, Q., Chang, C., & Zhang, L. (2018). Phase transition identification of
638 cellulose nanocrystal suspensions derived from various raw materials. *Journal of*
639 *Applied Polymer Science, 135*(24), 45702.
640 Zhu, J. Y., Sabo, R., & Luo, X. (2011). Integrated production of nano-fibrillated
641 cellulose and cellulosic biofuel (ethanol) by enzymatic fractionation of wood
642 fibers. *Green Chemistry, 13*(5), 1339.
643